nanomaterials

MDPI

Article

RETRACTED: Synthesis, Optical and Structural Properties of Copper Sulfide Nanocrystals from Single Molecule Precursors

Peter A. Ajibade * and Nandipha L. Botha

Department of Chemistry, University of Fort Hare, Private Bag X1314, Alice 5700, South Africa; 200904696@ufh.ac.za

* Correspondence: pajibade@ufh.ac.za; Tel.: +27-406022055; Fax: +27-865181225

Academic Editors: Shirley Chiang and Thomas Nann

Received: 5 August 2016; Accepted: 30 November 2016; Published: 4 February 2017

Abstract: We report the synthesis and structural studies of copper sulfide nanocrystals from copper (II) dithiocarbamate single molecule precursors. The precursors were thermolysed in hexadecylamine (HDA) to prepare HDA-capped CuS nanocrystals. The optical properties of the nanocrystals studied using UV–visible and photoluminescence spectroscopy showed absorption band edges at 287 nm that are blue shifted, and the photoluminescence spectra show emission curves that are red-shifted with respect to the absorption band edges. These shifts are as a result of the small crystallite sizes of the nanoparticles leading to quantum size effects. The structural studies were carried out using powder X-ray diffraction (XRD), transmission electron microscopy (TEM), scanning electron microscopy (SEM), energy dispersive X-ray spectroscopy (EDS), and atomic force microscopy. The XRD patterns indicates that the CuS nanocrystals are in hexagonal covellite crystalline phases with estimated particles sizes of 17.3–18.6 nm. The TEM images showed particles with almost spherical or rod shapes, with average crystallite sizes of 3–9.8 nm. SEM images showed morphology with ball-like microspheres on the surfaces, and EDS spectra confirmed the presence of CuS nanoparticles.

Keywords: CuS; dithiocarbamate; nanoparticles; electron microscopy; atomic force microscopy (AFM)

1. Introduction

The synthesis and studies of the optical and structural properties of nanomaterials expecially metal chalcogenides have received considerable attention in the last decades due to quantum confirement effects associated with their small crystallites sizes [1–6] that give them novel properties that make them useful in light-emitting diodes [7], solar cells [8], fuel cells [9], drug delivery [10,11], and as catalysts for industrial transformations [12–16]. Group 12 chalcogenides—especially ZnS [17,18] and CdS [19,20] nanoparticles have been widely studied but their toxicity limits any possible applications. As of result of the inherent toxicity of group 12 metal chalcogenides, copper sulfide nanocrystals are being explored for different applications [21–27]. CuS nanoparticle are also attractive because they exist in different stoichiometric compositions with varying crystalline phases [28–31].

Several methods have been used to synthesize metal sulfide nanoparticles, including solvothermal synthesis [32], microwave [33], ultrasonic irradiation [34], and thermolysis of single-source precursors in high boiling point solvents that act as surface passivating agents [35–38]. For the synthesis of CuS nanocrystals, different synthetic techniques have also been used [39–42] to produce nanoparticles with varying morphologies such as nanotubes [43], nanowires [44], and nanoplatelets [45], among others [46,47]. Among nanocrystal synthetic methods, the single-source precursor technique produces nanocrystals with reasonable monodispersity [48], and studies have indicated that the sizes and shapes of the resulting nanocrystals are influenced by the precursor concentration [49], reaction

This paper has been retracted. A Retraction notice was published on 14 December 2018 at *Nanomaterials* **2018**, *8*, 1047; doi:10.3390/nano8121047.

time [50], and temperature [51]. As a result of nanocrystals' unique size-dependent physical and chemical properties [52,53], the synthesis of monodisperse nanocrystals continue to attract much research attention [54]. In this paper, we report the use of three copper (II) dithiocarbamate complexes as efficient single-source precursors for the preparation of hexadecylamine (HDA)-capped copper sulfides nanoparticles. HDA was used as capping agent to passivate the sulface of the nanoparticles and prevent the particles from forming clump to larger particles. The optical and structural properties of the nanoparticles were studied using UV–visible, photoluminescence (PL), X-ray diffraction (XRD), transmission electron microscopy (TEM), scanning electron microscopy (SEM), energy dispersive X-ray spectroscopy (EDS) and atomic force microscopy (AFM).

2. Materials Methods

2.1. Materials and Physical Measurements

All chemicals and reagents were used as received without further purifications. Hexadecylamine (HDA), trioctylphosphine (TOP), toluene, and methanol are analytical-grade reagents used as obtained from Sigma-Aldrich (St. Louis, MO, USA). The ligands, sodium salt of *N*-phenyldithiocarbamate, *N*-ethylphenyldithiocarbamate, and morpholinedithiocarbamate were prepared using literature procedures [55,56]. Powder X-ray diffraction patterns were obtained from Bruker D8 Advance (Billerica, MA, USA) equipped with a proportional counter using Cu Kα radiation (λ = 1.5405 Å, nickel filter). TEM images were obtained from a ZEISS Libra 120 electron microscope (Oberkochen, Germany). Thermogravimetric analysis (TGA) was recorded on an SDTQ 600 thermogravimetric instrument (New Castle, DE, USA). The infrared spectra were obtained from a PerkinElmer Paragon 2000 Fourier-transform infrared (FTIR) spectrophotometer (Waltham, MA, USA) using the KBr disk method, UV–vis spectra were recorded on a PerkinElmer Lambda 25 UV–vis spectrophotometer (Waltham, MA, USA), and the photoluminescence study was recorded with PerkinElmer LS 45 fluorimeter (Waltham, MA, USA) (SEM was done using Jeol JSM-6390 LVSEM (Akishimo, Tokyo, Japan) at a rating voltage of 15–20 kV at different magnifications, as indicated on the SEM images. Energy dispersive spectra were processed using EDS attached to a Jeol, JSM-6390 LV SEM with Noran System *Six* software (Waltham, MA, USA). AFM was carried out using Digital Instruments Nanoscope, Veeco, MMAFMLN-AM (Multimode) (San Jose, CA, USA).

2.2. Synthesis of Copper (II) Dithiocarbamate Complexes

In a typical synthesis, a solution of $CuCl_2$ (0.625 mmol) was dissolved in 25 mL of water or methanol and added to 1.250 mmol of the sodium salt of *N*-phenyldithiocarbamate. Greenish brown precipitates formed immediately and the reaction mixture was stirred for 1 h at room temperature. The products were filtered and washed several times with water and methanol. The resulting copper (II)-*N*-phenyl dithiocarbamate complex [Cu(phendtc)$_2$] was dried at room temperature. A similar procedure was used for the synthesis of copper (II) complexes of *N*,*N*′-ethylphenyldithiocarbamate [Cu(ephendtc)$_2$] and morpholinedithiocarbamate [Cu(morpdtc)$_2$].

[Cu(phendtc)$_2$]: Selected IR (cm^{-1}): *v*(N–H) 3451, *v*(C–N) 1450, *v*(C–S) 1109, *v*(M–S) 328.
[Cu(ephendtc)$_2$]: Selected IR (cm^{-1}): *v*(N–H) 3417, *v*(C–N) 1472, *v*(C–S) 1067, *v*(M–S) 329.
[Cu(morpdtc)$_2$]: Selected IR (cm^{-1}): *v*(N–H) 3416, *v*(C–N) 1484, *v*(C–S) 1016, *v*(M–S) 327.

2.3. Synthesis of HDA-Capped CuS Nanoparticles

The metal sulfide nanoparticles were prepared by dissolving 0.20 g of each metal complex in 4 mL of TOP and injected into 3 g of hot HDA at 180 °C. An initial decrease of about 20–30 °C in temperature was observed. The solution was stabilized at 180 °C and the reaction continued for 1 h. After completion, the reaction mixture was allowed to cool to 70 °C, and methanol was added to precipitate the nanoparticles. The solid was separated by centrifugation and washed three times with methanol. The resulting solid precipitates of HDA-capped copper sulfide nanoparticles were dispersed in toluene

for further analysis. Synthesized CuS nanoparticles from copper (II) *N*-phenyldithiocarbamate complex is labeled **CuS1**; from copper (II) *N*,*N*-ethyl phenyldithiocarbamate complex is labeled **CuS2**, and from copper (II) morpholinedithiocarbamate complex is labeled **CuS3**.

3. Results and Discussion

3.1. Optical Properties of the CuS Nanoparticles

UV–vis spectrophotometry was used to study the absorption properties of the as-prepared nanoparticles. Figure 1 shows the absorption spectra of the CuS nanoparticles and reveals that the absorption band edges of **CuS1** and **CuS2** are almost similar and appear at about 287 nm. The absorption spectrum of **CuS3** differs slightly from the other two, with an absorption band edge at about 286 nm. The absorption spectra showed considerable blue-shift, which could be ascribed to the quantum size effect of the nanoparticles due to their smaller crystallite sizes [57,58]. The optical properties of semiconductor nanoparticles are strongly influenced by their crystallite sizes and shapes [59–62]. The calculated band gap energies for **CuS1** and **CuS2** are 4.33 eV. This value is greater than that of the bulk CuS, which is 1.2 eV [39]. **CuS3**, with absorption maxima at 286 nm and calculated band gap energy of 4.3 eV, is also blue-shifted and quantum confined. Figure 2 shows the photoluminescence spectra of the as-prepared CuS nanoparticles obtained at room temperature. The spectra are red-shifted intense but narrow-peaked at 620 nm. The observed red-shift could be attributed to the trap-related electron-hole recombination [51,52]. The spectra show that nanoparticles obtained from different precursors have the same emission maxima but differ in their intensity and peak widths. **CuS2** prepared from ($Cu(ephendtc)_2$) shows a narrow and sharp emission peak that is higher than the other two, indicating better electronic passivation of the **CuS2** nanoparticles by the capping agents. The reduced broadness of the emission curves can be attributed to their narrow size distributions. Although the absorption spectrum of **CuS3** is different from those of **CuS1** and **CuS2**, the emission spectra of the three nanoparticles are similar, differing only in their intensities.

3.2. Powder X-Ray Diffraction Analysis of the CuS Nanoparticles

XRD patterns for the nanocrystals prepared using different precursors are shown in Figure 3. The diffraction patterns showed four broad peaks that could be indexed to the hexagonal covellite crystalline phase of CuS with characteristic (101), (102), (103), and (006), and in good agreement with the standard data for CuS (JCPDS Card No. 06-0464) [63,64]. The average crystallite size of the nanoparticles, as estimated using Scherrer equation [65], are 18.09 nm for **CuS1**, 17.3 nm for **CuS2**, and 18.6 nm for **CuS3**, respectively.

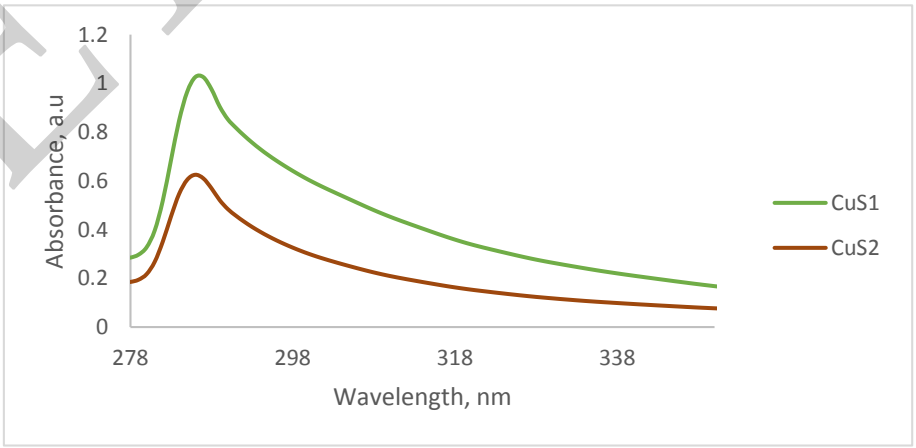

Figure 1. *Cont.*

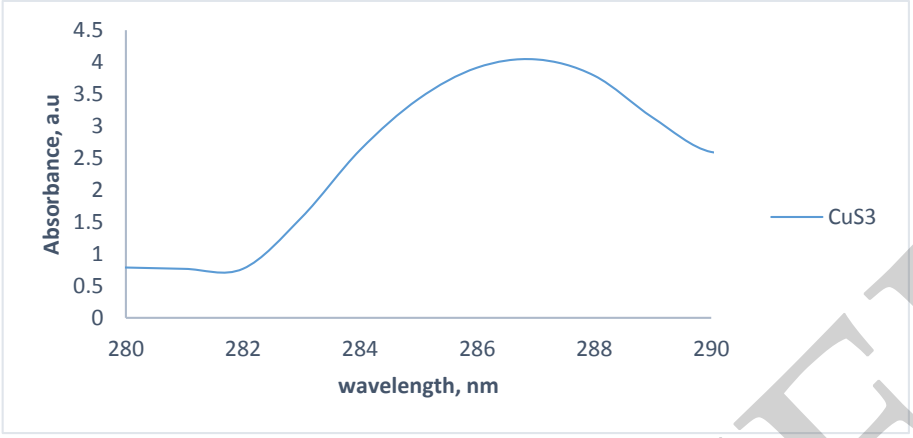

Figure 1. Absorption spectra of copper (II)-*N*-phenyl dithiocarbamate complex (**CuS1**), copper (II)-*N*,*N*-ethylphenyldithiocarbamate (**CuS2**), and copper (II)-morpholinedithiocarbamate (**CuS3**) nanoparticles.

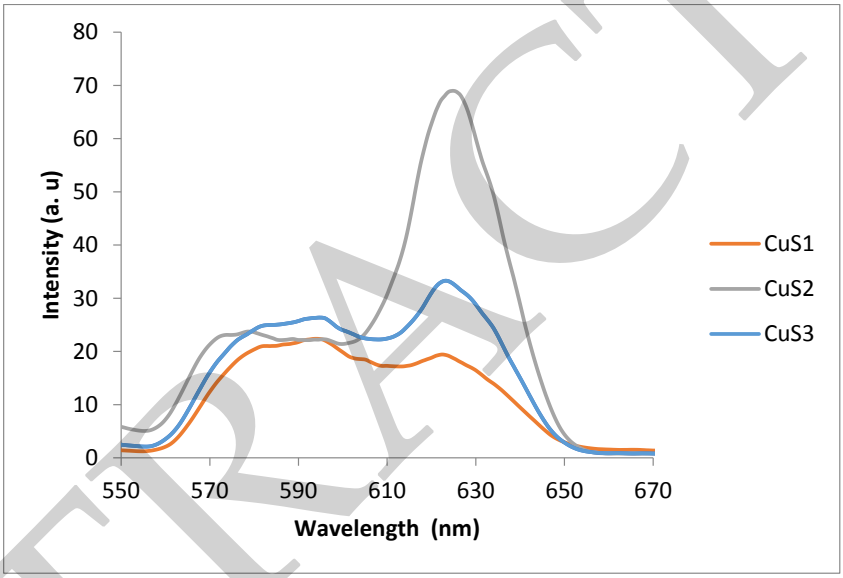

Figure 2. Emission spectra of **CuS1**, **CuS2**, and **CuS3** nanoparticles.

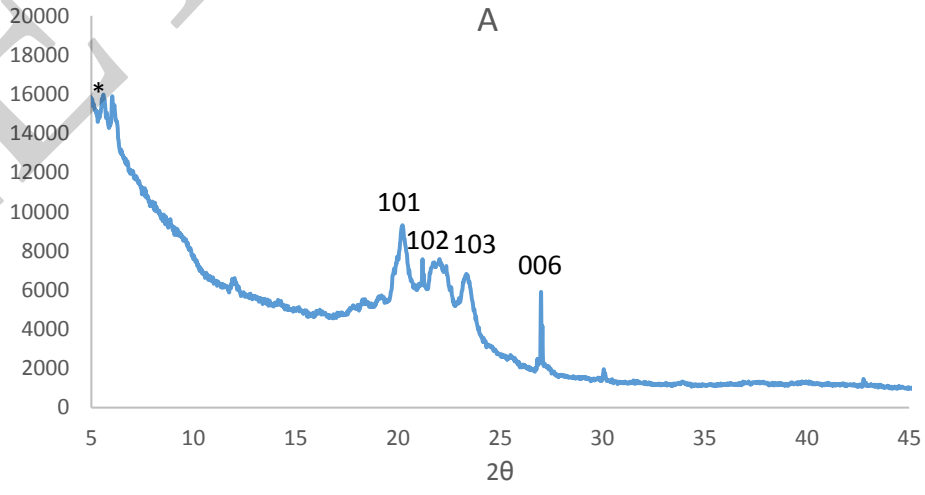

Figure 3. *Cont.*

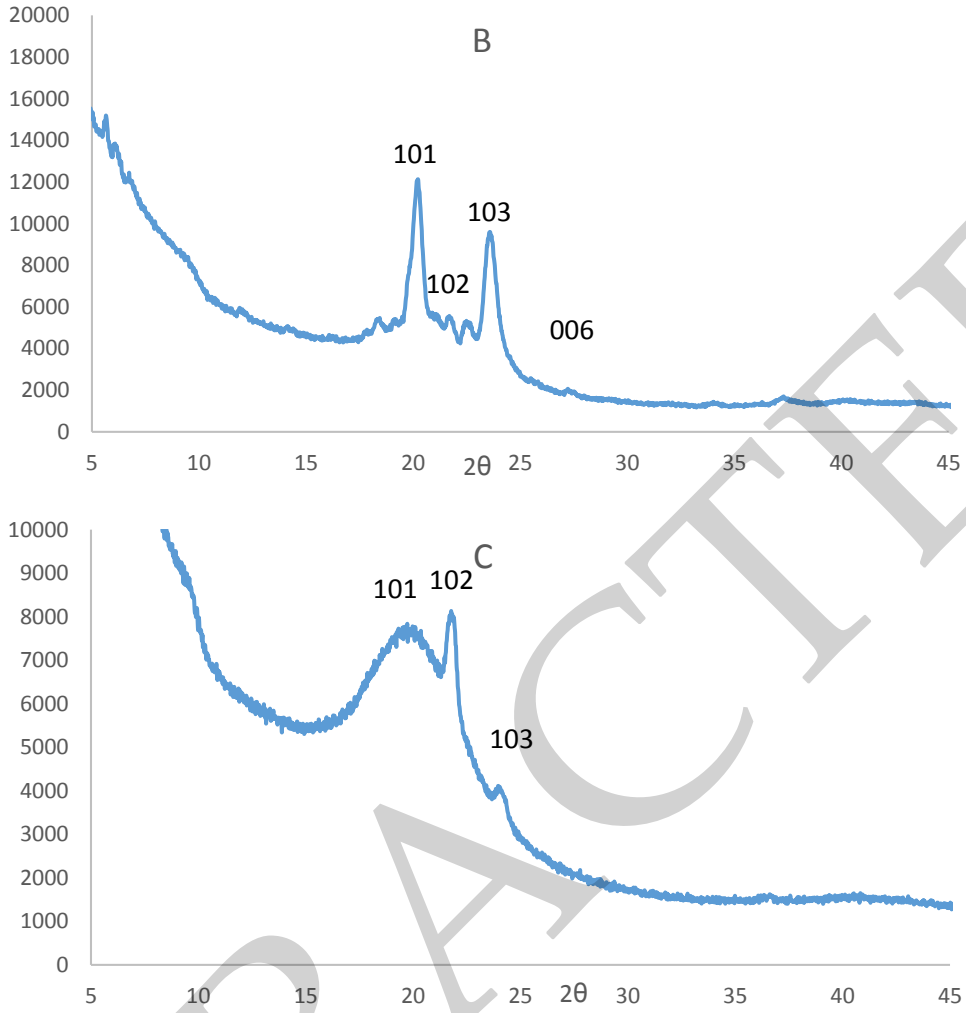

Figure 3. Powder X-ray diffraction (XRD) patterns of **CuS1** (**A**), **CuS2** (**B**), and **CuS3** (**C**) nanoparticles * hexadecylamine (HDA).

3.3. Morphology of the CuS Nanocrystals

The morphology and microstructure of the as-prepared CuS nanocrystals were studied with TEM, SEM, EDS, and AFM analyses. Figure 4 shows TEM images of the HDA-capped copper sulfide nanoparticles, which vary in shape from rodlike in **CuS1** to almost spherical and fairly monodispersed in **CuS2** and **CuS3**. The TEM image of **CuS1** shows copper sulfide nanoparticles with the average crystal size in the range of 5.10–9.80 nm, and its shapes appears to be a mixture of rodlike and some cubic-shaped nanoparticles. The TEM image of **CuS2** shows nanoparticles that are small, spherically shaped particles which are uniformly distributed, with the average crystallite size in the range 3.06–4.35 nm. The TEM image of **CuS3** shows small, spherically shaped nanoparticles with some aggregation. The crystallite sizes of the nanoparticles are in the range 3.02–4.32 nm.

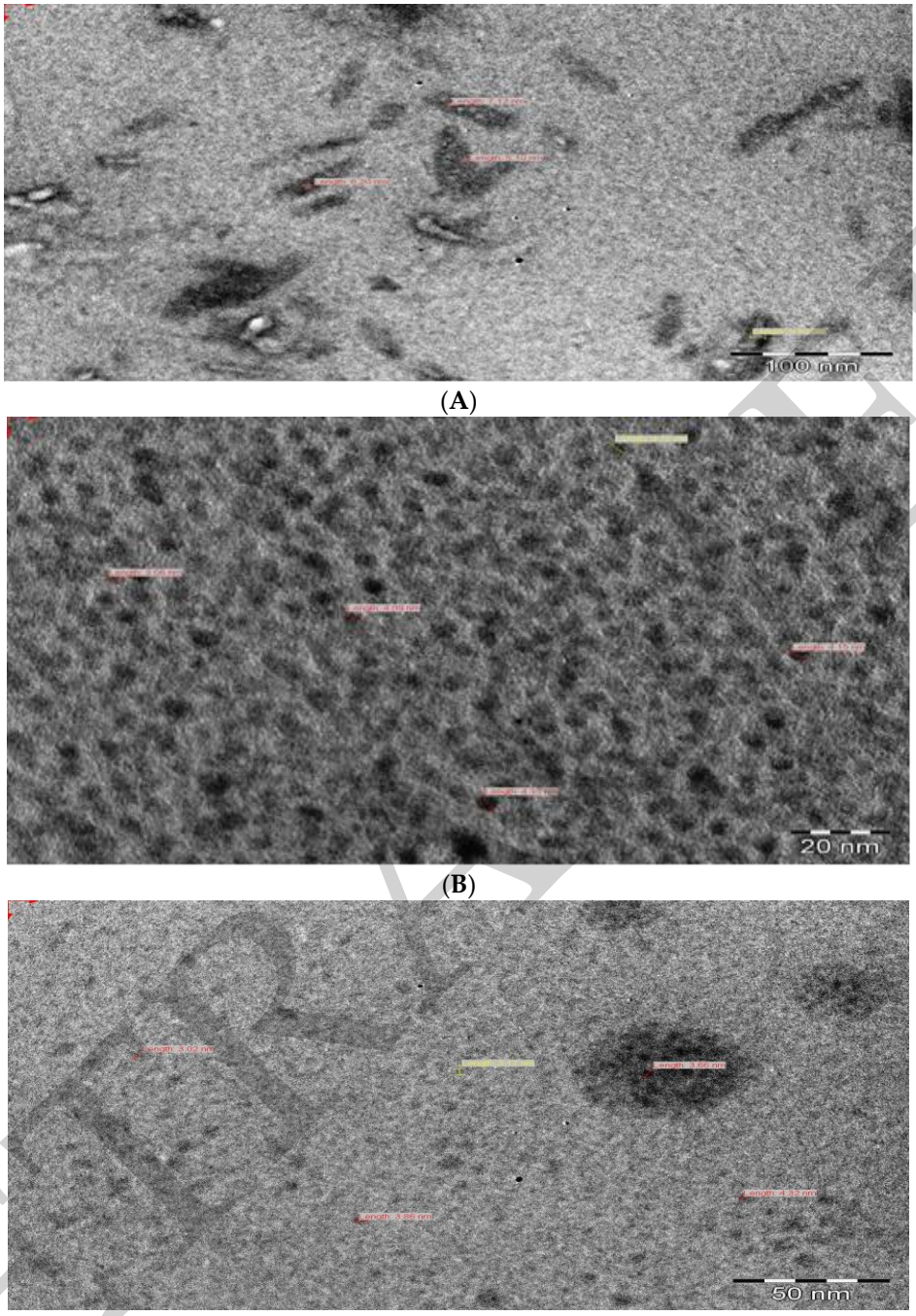

Figure 4. Transmission electron microscopy (TEM) images of **CuS1** (**A**), **CuS2** (**B**), and **CuS3** (**C**) nanoparticles.

The SEM images of the CuS nanoparticles and their elemental composition, as confirmed by EDS, are shown in Figure 5. It can be seen that the surface of the particles appears smooth with small microspheres on the surface. As expected, the microspheres on the surface are much bigger than that of the crystallite size measured by TEM analysis. This may be due to the agglomeration of crystallites occurring in the course of preparing the sample for SEM analyses. The EDS patterns show copper and sulfur, confirming the formation of CuS nanoparticles. Other peaks that seems to be common for all XRD spectra are phosphorus, nitrogen, and oxygen due to TOP that was used for dispersing the precursor and the HDA that was used as a capping agent.

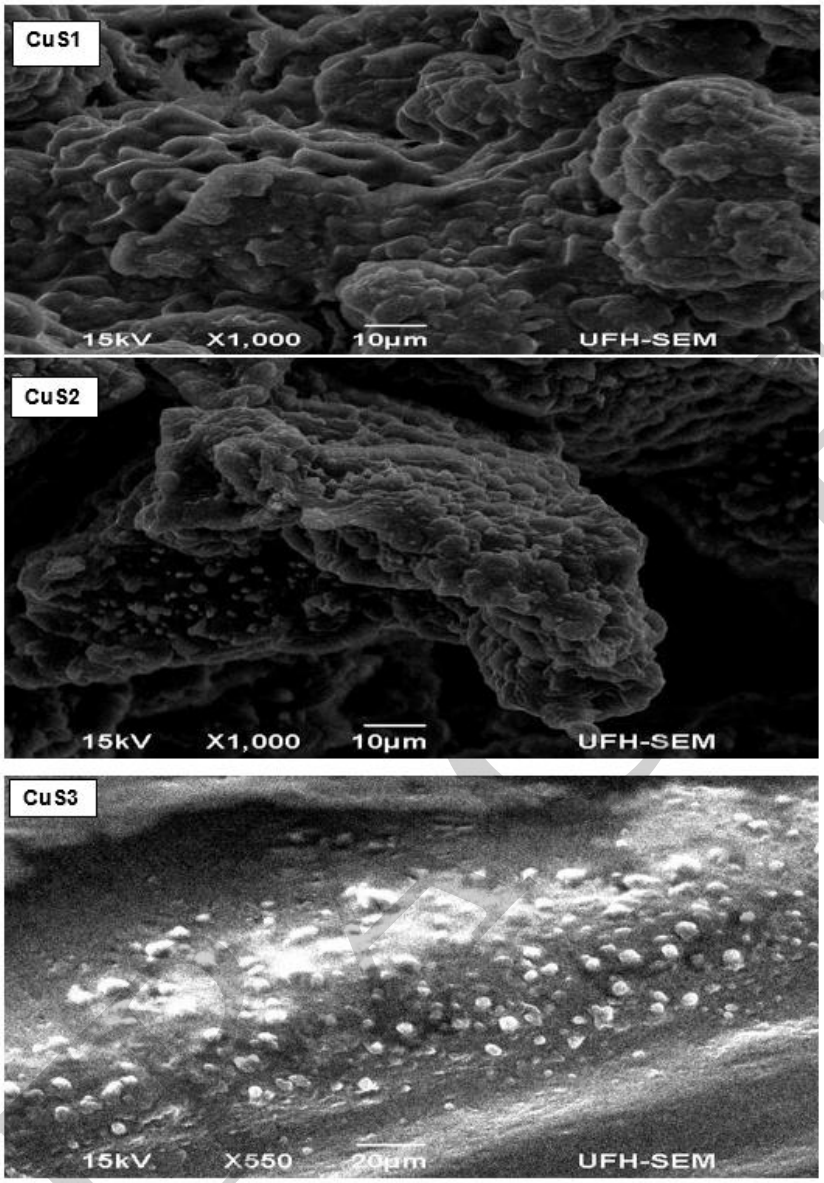

Figure 5. Scanning electron microscopy (SEM) images of **CuS1**, **CuS2**, and **CuS3** nanoparticles.

AFM was used to investigate the surface morphology and surface roughness [66,67]. AFM techniques provide microscopic and topographic information about the surface relief of the nanocrystals [67,68]. Thus, digital images for quantitative measurements of surface features such as three-dimensional simulation, average roughness (*R*a), and root mean square roughness (*R*q) can be obtained by AFM [66–69]. The topographical view of the nanoparticles (Figures 6–8) reveals that **CuS1** and **CuS3** nanoparticles are richer in dents and irregular surfaces than **CuS2**. The values of *R*q and *R*a were found to be 5.77 and 2.76 nm for **CuS1**; 24.8 and 18.9 nm for **CuS2**; and 12.6 and 9.00 nm for **CuS3**, respectively.

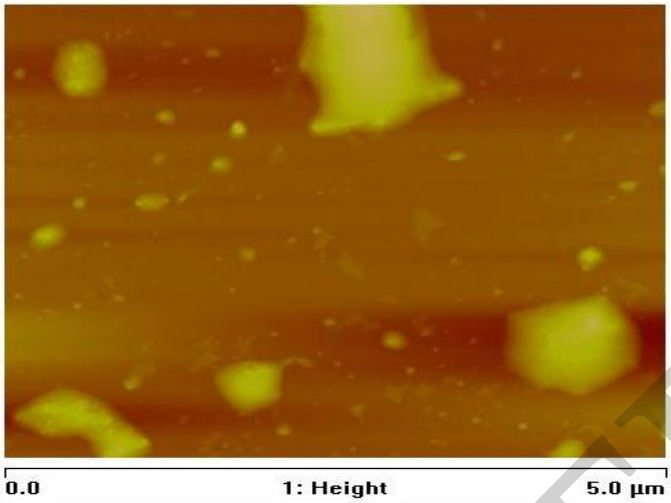

(**A**)

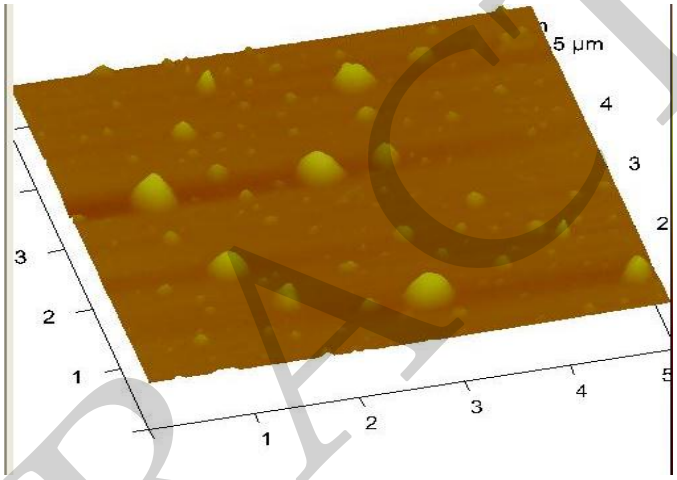

(**B**)

Figure 6. Atomic force microscopy (AFM) surface roughness (**A**) and 3D topographical images (**B**) of **CuS1** nanoparticles.

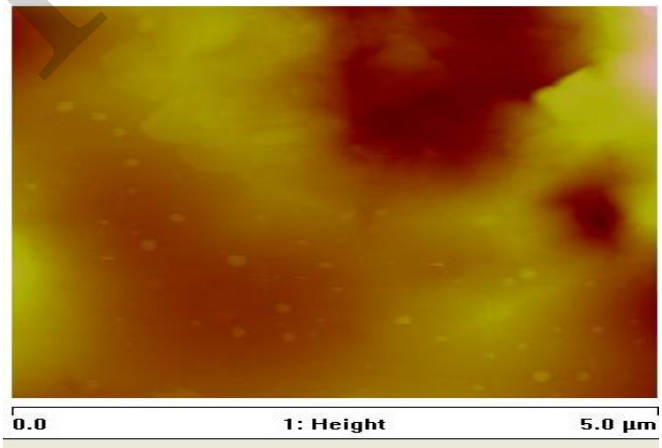

(**A**)

Figure 7. *Cont*.

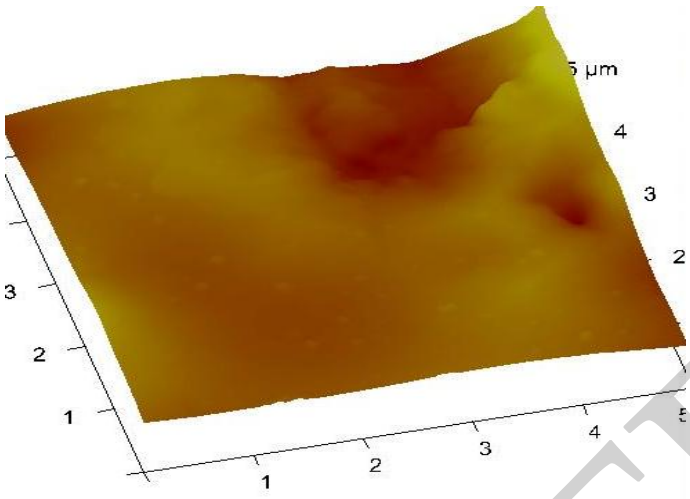

(**B**)

Figure 7. AFM surface roughness (**A**) and 3D topographical images (**B**) of **CuS2** nanoparticles.

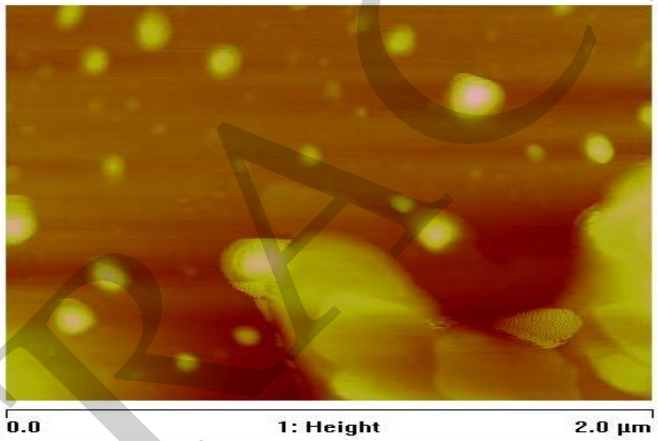

(**A**)

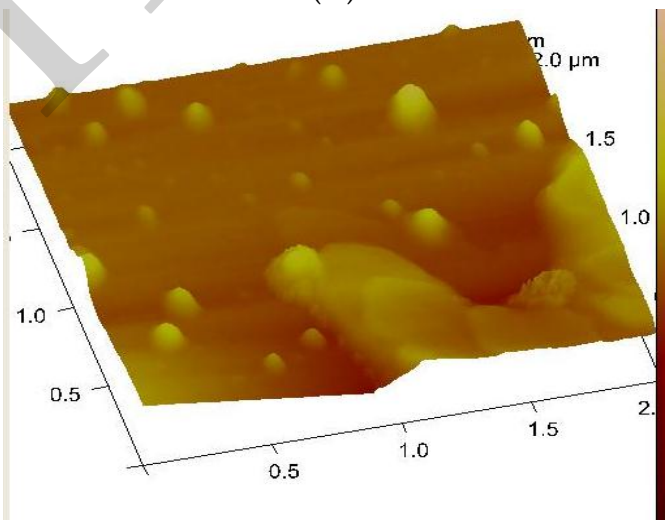

(**B**)

Figure 8. AFM surface roughness (**A**) and 3D topographical images (**B**) of CuS3 nanoparticles.

4. Conclusions

Copper (II) complexes of dithiocarbamate were used as single-source precursors to synthesize HDA-capped CuS nanoparticles. The optical studies showed that the absorption spectra of the as-prepared nanoparticles are blue-shifted and the emission maxima showed a narrower size distribution, which indicates a size quantum effect. The XRD patterns were indexed to the hexagonal CuS nanocrystals with estimated particle sizes of 17.3–18.6 nm. TEM images showed nanoparticles that are almost spherical in shape and fairly monodispersed, with average crystallite sizes of 3–9.8 nm.

Acknowledgments: The authors gratefully acknowledge the financial support of Govan Mbeki Research and Development Centre, University of Fort Hare, National Research Foundation, South Africa and ESKOM South Africa tertiary education support programme.

Author Contributions: N.L.B. and P.A.A. conceived and designed the experiments; N.L.B. performed the experiments; N.L.B. and P.A.A. analyzed the data; P.A.A. contributed reagents/materials/analysis tools; P.A.A. and N.L.B. contributed in writing the paper.

Conflicts of Interest: The authors declare no conflict of interest.

1. Antoniadou, M.; Daskalaki, V.M.; Balis, N.; Kondarides, D.I.; Kordulis, C.; Lianos, P. Photocatalysis and photoelectrocatalysis using (CdS-ZnS)/TiO_2 combined photocatalysts. *Appl. Catal.* **2011**, *107*, 188–196. [CrossRef]
2. Lai, C.H.; Lu, M.Y.; Chen, L.J. Metal sulfide nanostructures: Synthesis, properties and applications in energy conversion and storage. *J. Mater. Chem.* **2012**, *22*, 19–30. [CrossRef]
3. Kosyachenko, L.; Toyana, T. Current–voltage characteristics and quantum efficiency spectra of efficient thin-film CdS/CdTe solar cells. *Sol. Energy Mater. Sol. Cells* **2014**, *120*, 512–520. [CrossRef]
4. Wand, Z.H.; Geng, D.Y.; Zhang, Y.J.; Zhang, Z.D. CuS:Ni flowerlike morphologies synthesized by the solvothermal route. *Mater. Chem. Phys.* **2010**, *222*, 241–245.
5. Milliron, D.J.; Hughes, S.M.; Cui, Y.; Manna, L.; Li, J.B.; Wand, L.W.; Alivisatos, A.P. Colloidal nanocrystal heterostructures with linear and branched topology. *J. Nat.* **2004**, *430*, 190–195. [CrossRef] [PubMed]
6. Xu, J.Z.; Xu, S.; Geng, J.; Li, G.X.; Zhu, J.J. The fabrication of hollow spherical copper sulfide nanoparticle assemblies with 2-hydroxypropyl-β-cyclodextrin as a template under sonication. *Ultrason. Sonochem.* **2006**, *13*, 451–454. [CrossRef] [PubMed]
7. Kong, Y.L.; Tamargo, I.A.; Kim, H.; Johnson, B.N.; Gupta, M.K.; Koh, T.W.; Chin, H.A.; Steingart, D.A.; Rand, B.P.; McAlpine, M.C. 3D printed quantum dot light-emitting diodes. *Nano Lett.* **2014**, *14*, 7017–7023. [CrossRef] [PubMed]
8. Alberto, J.; Cllifford, J.N.; Palomares, E. Quantum dot based molecular solar cells. *Coord. Chem. Rev.* **2014**, *263–264*, 53–64. [CrossRef]
9. Gao, M.R.; Xu, Y.F.; Jiang, J.; Yu, S.H. Nanostructured metal chalcogenides: Synthesis, modification, and applications in energy conversion and storage devices. *Chem. Soc. Rev.* **2013**, *42*, 2986–3017. [CrossRef] [PubMed]
10. Couvreur, P. Nanoparticles in drug delivery: Past, present and future. *Adv. Drug Deliv. Rev.* **2013**, *65*, 21–23. [CrossRef] [PubMed]
11. Arias, J.L.; Reddy, L.H.; Othman, M.; Gillet, B.; Desmaele, D.; Zouhiri, F.; Dosio, F.; Gref, R.; Couvreur, P. Squalene based nanocomposites: A new platform for the design of multifunctional pharmaceutical theragnostics. *ACS Nano* **2011**, *22*, 1513–1521. [CrossRef] [PubMed]
12. Alivisatos, A.P. Semiconductor clusters, nanocrystals, and quantum dots. *Science* **1996**, *271*, 933–937. [CrossRef]
13. Wadia, C.; Alivisatos, A.P.; Kammen, D.M. Materials availability expands the opportunity for large-scale photovoltaics deployment. *Environ. Sci. Technol.* **2009**, *15–43*, 2072–2077. [CrossRef]
14. Xie, Y.L. Enhanced photovoltaic performance of hybrid solar cell using highly oriented CdS/CdSe-modified TiO_2 nanorods. *Electrochim. Acta* **2013**, *105*, 137–141. [CrossRef]
15. Safrani, T.; Jopp, J.; Golan, Y. A comparative study of the structure and optical properties of copper sulfide thin films chemically deposited on various substrates. *RSC Adv.* **2013**, *3*, 23066–23074. [CrossRef]

16. Nath, S.K.; Kalita, P.K. Chemical synthesis of copper sulfide nanoparticles embedded in PVA matrix. *Nanosci. Nanotechnol. Inter. J.* **2012**, *2*, 8–12.
17. Rao, B.S.; Kumar, B.R.; Reddy, V.R.; Rao, T.S. Preparation and characterization of CdS nanoparticles by chemical co-precipitation technique. *Chalco. Lett.* **2011**, *8*, 177–185.
18. Singh, V.; Chauhan, P. Synthesis and structural properties of wurtzite type CdS nanoparticles. *Chalco. Lett.* **2009**, *6*, 421–426.
19. Srinivasan, N.; Thirumaran, S.; Ciattini, S. Synthesis and crystal structures of diimine adducts of Cd(II) tetrahydroquinolinedithiocarbamate and use of (1,10-phenanthroline)bis(1,2,3,4-tetrahydroquinolinecarbodithioato-S,S′)-cadmium(II) for the preparation of CdS nanorods. *J. Mol. Struct.* **2012**, *1026*, 102–107. [CrossRef]
20. Mondal, G.; Bera, P.; Santra, A.; Jana, S.; Mandal, T.N.; Mondal, A.; Seok, S.; Bera, P. Precursor-driven selective synthesis of hexagonal chalcocite (Cu_2S) nanocrystals: Structural, optical, electrical and photocatalytic properties. *New J. Chem.* **2014**, *38*, 4774–4782. [CrossRef]
21. Soomro, R.A.; Sherazi, S.T.H.; Memon, S.N.; Shah, M.R.; Kalwar, N.H.; Hallam, K.R.; Shah, A. Synthesis of air stable copper nanoparticles and their use in catalysis. *Adv. Mater. Lett.* **2014**, *5*, 191–198. [CrossRef]
22. Kanhed, P.; Birla, S.; Gaikwad, S.; Gade, A.; Seabra, A.B.; Rubilar, O.; Duran, N.; Rai, M. In vitro antifungal efficacy of copper nanoparticles against selected crop pathogenic fungi. *Mater. Lett.* **2014**, *115*, 13–17. [CrossRef]
23. Guo, L.; Panderi, I.; Yan, D.D.; Szulak, K.; Li, Y.; Chen, Y.; Ma, H.; Niesen, D.B.; Seeram, N.; Ahmed, A.; et al. A comparative study of hollow copper sulfide nanoparticles and hollow gold nanospheres on degradability and toxicity. *Chem. Soc.* **2013**, *7*, 8780–8793. [CrossRef] [PubMed]
24. Dutta, A.K.; Das, S.; Samanta, S.; Partha, K.S.; Adhikary, B.; Biswas, P. CuS nanoparticles as amimic peroxidase for colorimetric estimation of human blood glucose level. *Talanta* **2013**, *107*, 361–367. [CrossRef] [PubMed]
25. Abdullaeva, Z.; Omurzak, E.; Mashimo, T. Synthesis of copper sulfide nanoparticles by pulsed plasma in liquid method. *World Acad. Int. Sch. Sci. Res. Innov.* **2013**, *7*, 422–425.
26. Kundu, J.; Pradhan, D. Influence of precursor concentration, surfactant and temperature on the hydrothermal synthesis of CuS: Structural, thermal and optical properties. *New J. Chem.* **2013**, *37*, 1470–1478. [CrossRef]
27. Pathana, H.M.; Desain, J.D.; Lokhande, C.D. Modified chemical deposition and physico-chemical properties of copper sulphide (Cu_2S) thin films. *Appl. Surf. Sci.* **2002**, *202*, 47–56. [CrossRef]
28. Zhang, P.; Gao, L. Copper sulfide flakes and nanodisks. *J. Mater. Chem.* **2003**, *13*, 2007–2010. [CrossRef]
29. Tan, C.; Zhu, Y.; Lu, R.; Xue, P.; Bao, C.; Liu, X.; Fei, Z.; Zhao, Y. Synthesis of copper sulfide nanotube in the hydrogel system. *Mater. Chem. Phys.* **2005**, *91*, 44–47. [CrossRef]
30. Zhang, W.; Wen, X.; Yang, S. Synthesis and characterization of uniform arrays of copper sulfide nanorods coated with nanolayers of polypyrrole. *Langmuir* **2003**, *19*, 4420–4426. [CrossRef]
31. Ghahremaninezhad, A.; Asselin, E.; Dixon, D.G. Electrodeposition and growth mechanism of copper sulfide nanowires. *J. Phys. Chem.* **2011**, *115*, 9320–9334. [CrossRef]
32. Park, J.; Joo, J.; Kwon, S.G.; Jang, Y.; Hyeon, T. Synthesis of monodisperse spherical nanocrystals. *Angew. Chem. Int. Ed.* **2007**, *46*, 4630–4660. [CrossRef] [PubMed]
33. Wada, Y.; Kuramoto, H.; Anand, J.; Kitamura, T.; Sakata, T.; Mori, H.; Yanagida, S. Microwave-assisted size control of CdS nanocrystallites. *J. Mater. Chem.* **2001**, *11*, 1936–1940. [CrossRef]
34. Ghows, N.; Entezari, M.H. A novel method for the synthesis of CdS nanoparticles without surfactant. *Ultrason. Sonochem.* **2011**, *18*, 269–275. [CrossRef] [PubMed]
35. Sohrabnezhad, S.H.; Pourahmad, A. CdS semiconductor nanoparticles embedded in AlMCM-41 by solid-state reaction. *J. Alloys Compd.* **2010**, *505*, 324–327. [CrossRef]
36. Nirmal, R.M.; Pandian, K.; Sivakumur, K. Cadmium (II) pyrrolidine dithiocarbamate complex as single source precursor for the preparation of CdS nanocrystals by microwave irradiation and conventional heating process. *Appl. Surf. Sci.* **2011**, *257*, 2745–2751. [CrossRef]
37. Trindade, T.; O'Brien, P. Synthesis of CdS and CdSe Nanocrystallites Using a Novel Single-Molecule Precursors Approach. *Chem. Mater.* **1997**, *9*, 523–530. [CrossRef]
38. Zhang, Y.C.; Wang, G.Y.; Hu, X.Y. Solvothermal synthesis of hexagonal CdS nanostructures from a single-source molecular precursor. *J. Alloys Compd.* **2007**, *437*, 47–52. [CrossRef]
39. Huang, Y.; Xiao, H.; Chen, S.; Wang, C. Preparation and characterization of CuS hollow spheres. *Cer Inter* **2009**, *35*, 905–907. [CrossRef]

40. Dhassade, S.S.; Patil, J.S.; Han, S.H.; Rath, M.C.; Fulari, V.J. Copper sulfide nanorods grown at room temperature for photovoltaic application. *Mater. Lett.* **2013**, *90*, 138–141. [CrossRef]
41. Maji, S.K.; Mukherjee, N.; Dutta, A.K.; Srivastaca, D.N.; Paul, P.; Karmakar, B.; Mondal, A.; Adhikary, B. Deposition of nanocrystalline CuS thin film from a single precursor: Structural, optical and electrical properties. *Mater. Chem. Phys.* **2011**, *130*, 392–397. [CrossRef]
42. Ma, G.; Zhou, Y.; Li, X.; Sun, K.; Liu, S.; Hu, J.; Kotov, N.A. Self-assembly of copper sulfide nanoparticles into nanoribbons with continuous crystallinity. *ACS Nano* **2013**, *7*, 9010–9018. [CrossRef] [PubMed]
43. Zhang, H.T.; Wu, G.; Chen, X.H. Controlled synthesis and characterization of covellite (CuS) nanoflakes. *Mater. Chem. Phys.* **2006**, *98*, 293–303.
44. Wu, C.; Shi, J.B.; Chen, C.J.; Chen, Y.C.; Lin, Y.T.; Wu, P.F.; Wei, S.Y. Synthesis and optical properties of CuS nanowires fabricated by electrodeposition with anodic alumina membrane. *Mater. Lett.* **2008**, *62*, 1074–1077. [CrossRef]
45. Liu, J.; Xue, D.F. Solvothermal synthesis of CuS semiconductor hollow spheres based on a bubble template route. *J. Cryst. Growth* **2009**, *311*, 500–503. [CrossRef]
46. Thongtem, T.; Phuruangrat, A.; Thongstem, S. Formation of CuS with flower-like, hollow spherical, and tubular structures using the solvothermal-microwave process. *Curr. Appl. Phys.* **2009**, *9*, 195–200. [CrossRef]
47. Tan, C.H.; Lu, R.; Xue, P.C.; Bao, C.Y.; Zhao, Y.Y. Synthesis of CuS nanoribbons templated by hydrogel. *Mater. Chem. Phys.* **2008**, *112*, 500–503. [CrossRef]
48. Pradhan, N.; Katz, B.; Efrima, S. Synthesis of High-Quality Metal Sulfide Nanoparticles from Alkyl Xanthate Single Precursors in Alkylamine Solvents. *J. Phys. Chem. B* **2003**, *107*, 13843–13854. [CrossRef]
49. Mondal, G.; Acharjya, M.; Santra, A.; Bera, P.; Jana, S.; Pramanik, N.C.; Mondal, A.; Bera, P. A new pyrazolyl dithioate function in the precursor for the shape controlled growth of CdS nanocrystals: Optical and photocatalytic activities. *New J. Chem.* **2015**, *39*, 9487–9497. [CrossRef]
50. Flor, J.; Marques de Lima, S.A.; Davalos, M.R. Effect of reaction time on the particle size of ZnO and ZnO:Ce obtained by a sol-gel method. *Prog. Colloid Polym. Sci.* **2004**, *128*, 239–243.
51. Sharma, K.N.; Joshi, H.; Prakash, O.; Sharma, A.K.; Bhaskar, R.; Singh, A.K. Pyrazole-Stabilized Dinuclear Palladium (II) Chalcogenolates Formed by Oxidative Addition of Bis [2-(4-bromopyrazol-1-yl) ethyl] Dichalcogenides to Palladium (II)–Tailoring of Pd–S/Se Nanoparticles. *Eur. J. Inorg. Chem.* **2015**, *29*, 4829–4838. [CrossRef]
52. Deori, K.; Ujjain, S.K.; Sharma, R.K.; Deka, S. Morphology controlled synthesis of nanoporous Co_3O_4 nanostructures and their charge storage characteristics in supercapacitors. *ACS Appl. Mater. Interfaces* **2013**, *5*, 10665–10672. [CrossRef] [PubMed]
53. Coe, S.; Woo, W.K.; Bawendi, M.; Bulovic, Y. Electroluminescence from single monolayers of nanocrystals in molecular organic devices. *Nature* **2002**, *420*, 800–803. [CrossRef] [PubMed]
54. Bera, P.; Kim, C.H.; Seok, S.I. Synthesis of nanocrystalline CdS from cadmium (II) complex of S-benzyl dithiocarbazate as a precursor. *Solid State Sci.* **2010**, *12*, 1741–1747. [CrossRef]
55. Kuo, C.H.; Chu, Y.T.; Song, Y.F.; Huang, M.H. Cu_2O nanocrystal-templated growth of Cu_2S nanocages with encapsulated Au nanoparticles and in-situ transmission X-ray microscopy study. *Adv. Funct. Mater.* **2011**, *21*, 792–797. [CrossRef]
56. Ajibade, P.A.; Benjamin, C.E. Group 12 dithiocarbamate complexes: Synthesis, spectral studies and their use as precursors for metal sulfides nanoparticles and nanocomposites. *Spectrochim. Acta A* **2013**, *113*, 408–414. [CrossRef] [PubMed]
57. Mthethwa, T.; Pullabhotla, V.S.R.; Mdluli, P.S.; Wesley-Smith, J.; Revaprasadu, N. Synthesis of hexadecylamine capped CdS nanoparticles using heterocyclic cadmium dithiocarbamates as single source precursors. *Polyhedron* **2009**, *28*, 2977–2982. [CrossRef]
58. Efros, A.L.; Rosen, M. Electronic structure of semiconductor nanocrystals. *Ann. Rev. Mater. Sci.* **2000**, *30*, 475–521. [CrossRef]
59. Donega, C.D.M. Synthesis and properties of colloidal heteronanocrystals. *Chem. Soc. Rev.* **2011**, *40*, 1512–1546. [CrossRef] [PubMed]
60. Kvitek, O.; Siegel, J.; Hnatowicz, V.; Svorlik, V. Noble metal nanostructures influence of structure and environment on their optical properties. *J. Nanomater.* **2003**, *2013*, 1–15. [CrossRef]
61. Gupta, P.; Ramrakhiani, M. Influence of the particle size on the optical properties of CdSe nanoparticles. *Open Nanosci. J.* **2009**, *3*, 15–19. [CrossRef]

62. Chandran, A.; Francis, N.; Jose, T.; George, K.C. Synthesis, structural characterization and optical band gap determination of ZnS nanoparticles. *SB Acad. Rev.* **2010**, *XVII*, 17–21.
63. Alivisatos, A.P. Perspectives on the physical chemistry of semiconductor. *Nanocryst. J. Phys. Chem.* **1996**, *100*, 13226–13239. [CrossRef]
64. Mercy, A.; Selvaraj, R.S.; Boaz, B.M.; Anandhi, A.; Kanagadurai, R. Synthesis, structural and optical characterization of cadmium sulphide nanoparticles. *Indian J. Pure Appl. Phys.* **2013**, *51*, 448–452.
65. Botha, N.L.; Ajibade, P.A. Effects of temperature on crystallite sizes of copper sulfide nanocrystals prepared from copper(II) dithiocarbamate single source precursors. *Mater. Sci. Semicond. Process.* **2016**, *43*, 149–154. [CrossRef]
66. Nabiyounil, G.; Sahraei, R.; Toghiany, M.; Mayles, M.; Hedayali, K. Preparation and characterization of nanostructured ZnS thin films grown on glass and N-type Si substrates using a new chemical bath deposition technique. *Rev. Adv. Mater. Sci.* **2011**, *27*, 52–57.
67. Al-Rasoul, K.T.; Abbas, N.K.; Shanam, S.J. Structural and optical characterization of Cu and Ni doped ZnS nanoparticles. *Int. J. Electorchem. Sci.* **2013**, *8*, 5594–5604.
68. Martinez, M.A.; Guillen, C.; Herrero, J. Morphological and structural studies of CBD-CdS thin films by microscopy and diffraction techniques. *Appl. Surf. Sci.* **1998**, *136*, 8–16. [CrossRef]
69. Martinez, M.A.; Guillen, C.; Herrero, J. Cadmium sulphide growth investigations on different SnO_2 substrates. *Appl. Surf. Sci.* **1999**, *140*, 182–189. [CrossRef]